Supplementary Information for:

Hydrocarbon-based membranes cost-effectively manage species transport and increase performance in thermally regenerative batteries

Nicholas R. Cross[a], Holkan V. Sanchez[b], Matthew J. Rau[c], Serguei N. Lvov[d,e,f], Michael A. Hickner[g], Christopher A. Gorski[h], S. Mani Sarathy[b], Bruce E. Logan[a,h] , Derek M. Hall[d,e 1]

[a]Department of Chemical Engineering, Pennsylvania State University, University Park, PA 16802, USA
[b]Department of Chemical and Biological Engineering, King Abdullah University of Science and Technology, Thuwal 23955, Saudi Arabia
[c]Department of Mechanical & Aerospace Engineering, George Washington University, Washington, DC 20052, USA
[d]The EMS Energy Institute, Pennsylvania State University, University Park, PA 16802, USA
[e]Department of Energy and Mineral Engineering, Pennsylvania State University, University Park, PA 16802, USA
[f]Department of Materials Science and Engineering, Pennsylvania State University, University Park, PA 16802, USA
[g]Department of Chemical & Materials Science Engineering, Michigan State University, East Lansing, MI 48824, USA
[h]Department of Civil and Environmental Engineering, Pennsylvania State University, University Park, PA 16802, USA
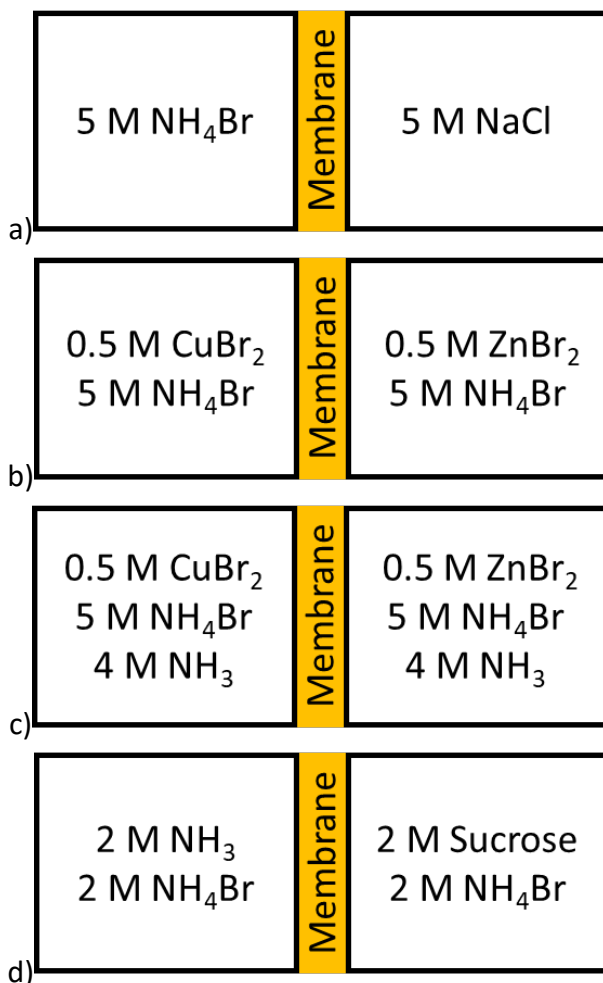
Figure S1: Schematics showing the electrolytes used for diffusion tests for determining flux of a) ammonium and bromide, b) copper bromide, c) copper ammonia, and d) ammonia. The source

[1] Corresponding author: dmh5373@psu.edu

electrolyte is always on the left and the sink electrolyte is on the right. Lower concentrations were used for ammonia tests due to the low solubility of the components in the sink electrolyte.
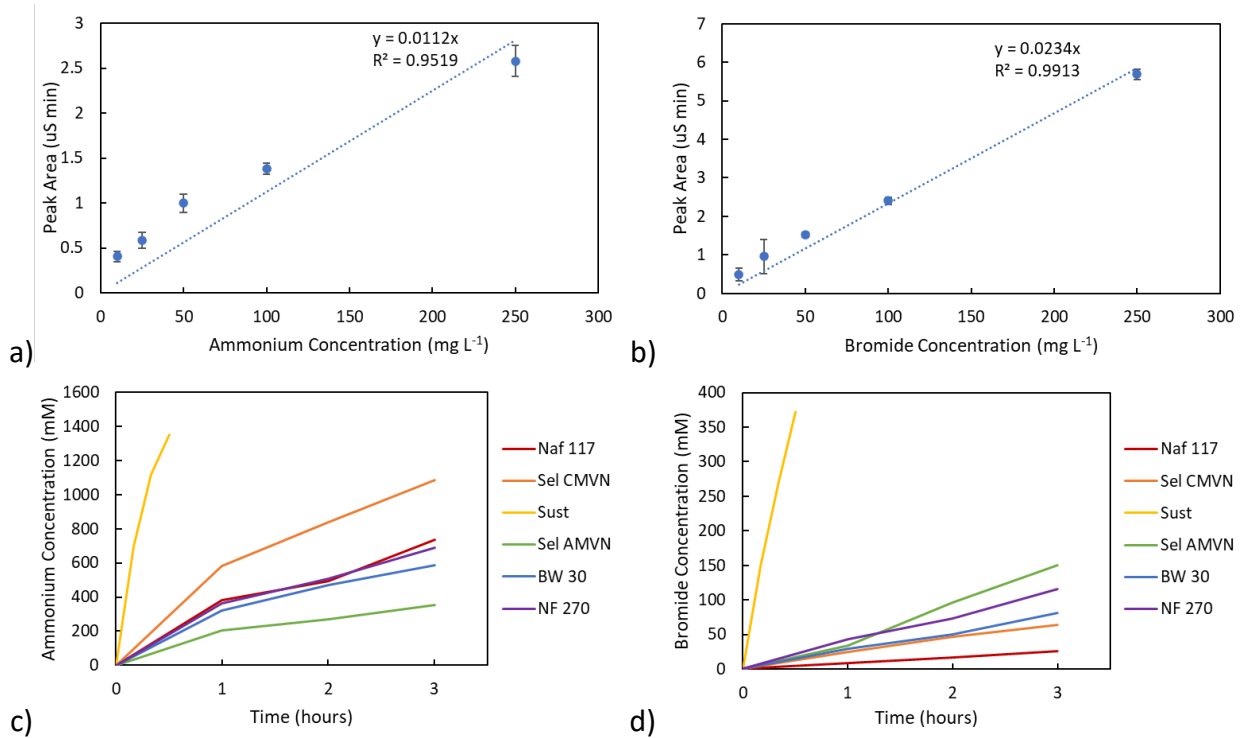

a) b)

c) d)

Figure S2: Calibration curves for ion chromatography tests of a) ammonium and b) bromide. Points and error bars are average and standard deviation of four trials. Calculated concentration of c) ammonium and d) bromide over time. The concentrations shown are averages of three trials.
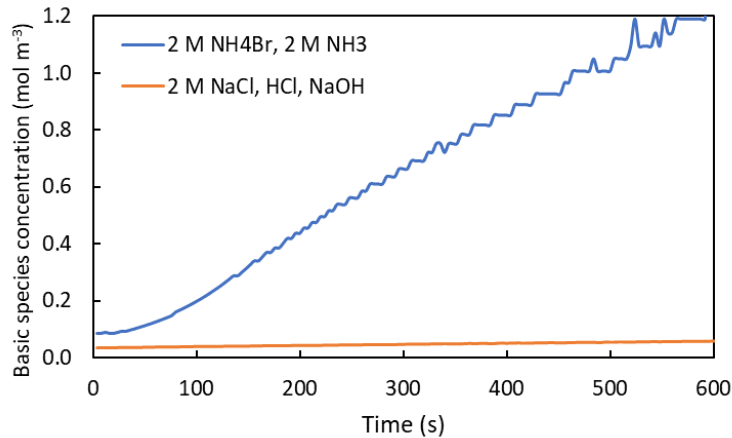

Figure S3: Comparison of change in basic species concentration for the "standard" test of 2 M NH$_4$Br and 2 M NH$_3$ as source electrolyte and 2 M NH$_4$Br and 2 M Sucrose as the sink electrolyte to a "hydronium/hydroxide" test with 2 M NaCl as the background salt in both electrolytes and NaOH added to the source electrolyte and HCl added to the sink electrolyte to create a similar pH gradient without the ammonia/um species.

Note: Flux from the "standard" test was 2.4 x 10^{-5} mol m^{-2} s^{-1} and flux from the "hydronium/hydroxide" test was 1.9 x 10^{-6} mol m^{-2} s^{-1}. Test was run with Selemion AMVN.

Table S1: Parameters and values used for the economic analysis.

| O&M/Discharging Parameters	Value	
	Power applications	Energy applications
Power capacity	1 MW	10 MW
Discharge time	0.02 h – 0.5 h	1 h – 15 h
Cycles per year	13000	250
Depth-of-discharge	100 %	
Round-trip efficiency (η_{RT})	73 %	
Cycle degradation	0.0027 % cycle^{-1}	
Time degradation	1.70 % year^{-1}	
Self-discharge (η_{self})	0 % day^{-1}	
Lifetime project	20 years	
Construction time	1 year	
Discount rate	6%	
Capital Costs	*Cost*	
Electrolyte tank	0.41 $ gal^{-1}	
Copper (II) bromide ($CuBr_2$)	0.0215 $ gal^{-1}	
Ammonium bromide (NH_4Br)	0.0095 $ g^{-1}	
Ammonium hydroxide (H_5NO @ 28%)	0.001 $ mL^{-1}	
Graphite felt electrode	0.007 $ cm^{-2}	
Rubber gaskets	0.0169 $/in^2	
Graphite plates with flow fields	30. $ m^{-2}	
End plates	0.0405 $ in^{-2}	
Pumps	18 $ gal^{-1} min^{-1}	
Tubing	0.08 $ m^{-1}	
Valves	0.40 $ piece^{-1}	
Power conditioning system (PCS)	210. $ kW^{-1}	
Distillation column (1000 ml)	19.475 $ L^{-1}	
Power	12 $ kW-yr^{-1}	
Energy	1 $ MWh^{-1}	
Charging cost	0	
End-of-life cost	0	
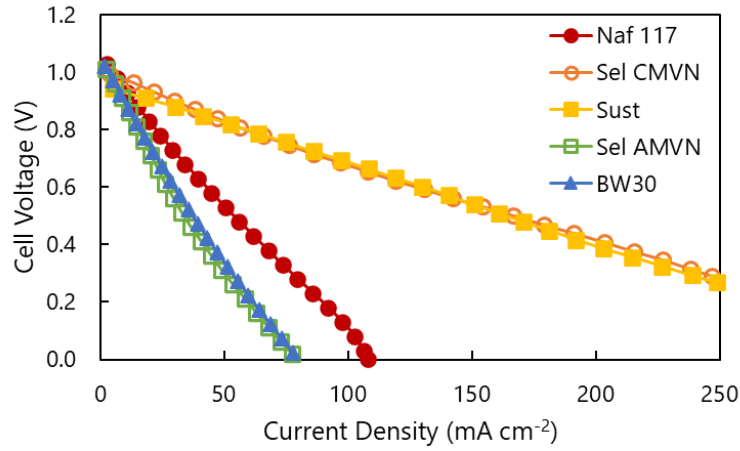
**Figure S4:** Polarization curves for each membrane studied in the full cell assembly.

Heat exchanger power density, ρ, was estimated as [1]

$$\rho = \eta_* U \Delta T_{he} \left(1 - \frac{\Delta T_*}{T_H - T_L} \right)$$
(1)

where η_* is the modified energy efficiency, U is the heat transfer coefficient (1000 W m^{-2} K^{-1}), ΔT_{he} is the heat exchanger temperature gradient (5 K), and ΔT_* is the temperature difference across a single TRAB thermal recharging unit (75 °C).

Table S2: Heat exchanger power density of the Cu$_{aq}$-TRAB with Selemion CMVN at different applied current densities.

Current Density (mA cm^{-2})	10	30	50	100
ρ (W m^2)	39	34	31	16

a)

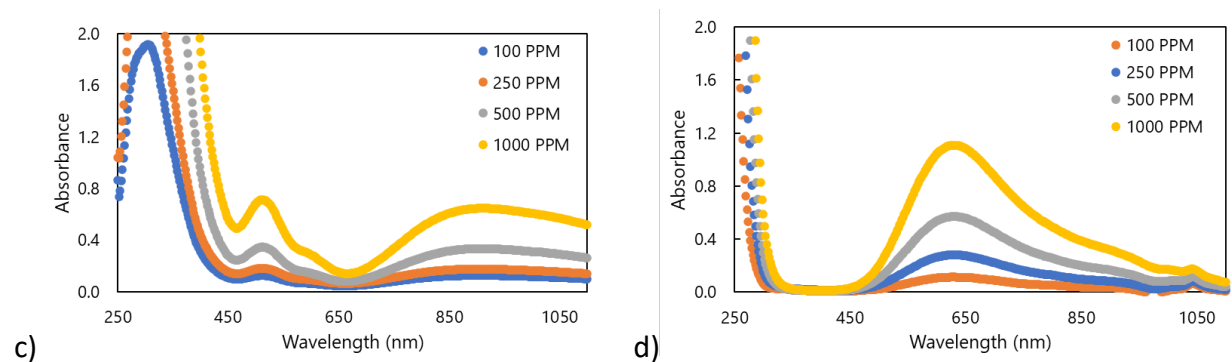
b)

c)   d)
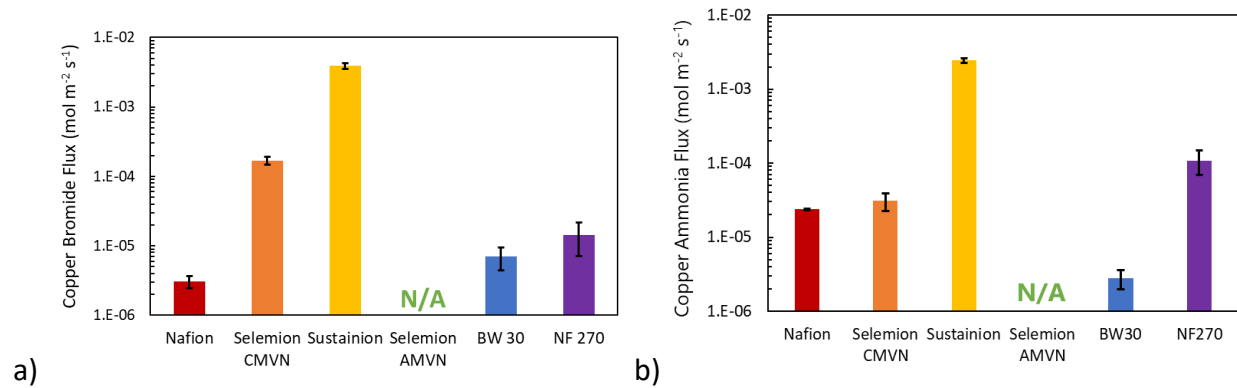
Figure S5: Flux of a) copper(II) bromide and b) copper(II) ammonia through each membrane. Copper species were not detected in the sink electrolyte after 72 hours of testing for Selemion AMVN. UV-Vis spectra of c) copper (II) bromide solutions and d) copper (II) ammonia solutions at a range of concentrations used to create calibration curves for estimation of copper species flux. Peaks at 512 and 900 nm were used for copper (II) bromide and the peak at 626 nm was used for copper(II) ammonia.
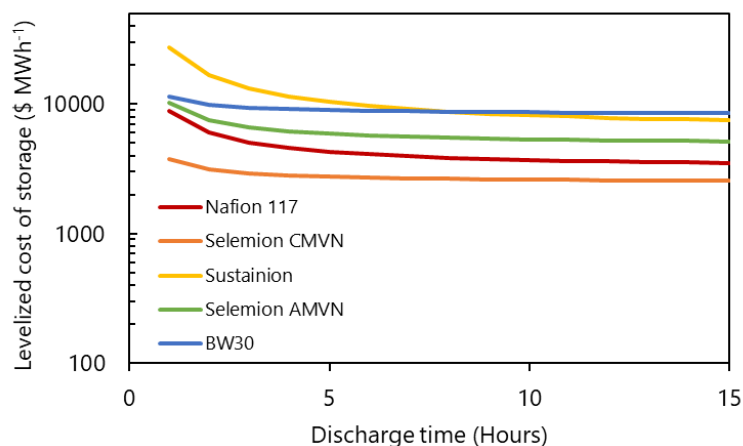

Figure S6: LCOS of the Cu_{aq}-TRAB for long-term energy storage applications with all membranes studied. The power density used was 30% of the peak power and the energy density was the same as experimentally measured (**Figure 2a and b**).

References

[1]   D. Brogioli, F. La Mantia, Electrochemical Methods for Exploiting Low-Temperature Heat Sources: Challenges in Material Research, Adv. Energy Mater. 12 (2022) 2103842. https://doi.org/10.1002/aenm.202103842.